ARTICLE OPEN

Check for updates

Cooperative-effect-induced one-way steering in open cavity magnonics

Si-Yu Guan[1], Hong-Fu Wang[1,2]✉ and Xuexi Yi[1]✉

We propose to generate and control stationary one-way steering with strong entanglement between photon and magnon modes by the cooperative effect of coherent coupling and dissipative coupling. Due to the combination of two couplings, the system becomes a parity-time-like symmetric non-Hermitian system, and two exceptional points (EPs)-like appear in the real and imaginary parts of the eigenvalues. We demonstrate that the especially obvious quantum entanglement and perfect one-way steering can be obtained around two EPs-like. The continuous variable entanglement and steering produced by this cooperative effect show stronger robustness to environment temperature and system dissipation than that induced by nonlinearity. The one-way steering directivity can be controlled by the relative phase of cooperative dissipation and the frequency detuning of the magnon mode. Our work shows the controllability advantage of the open cavity magnonic system and may open up a platform for the generation of stationary one-way steering.

npj Quantum Information (2022)8:102 ; https://doi.org/10.1038/s41534-022-00619-y

INTRODUCTION

Quantum entanglement and Bell nonlocality, as the core of quantum information theory, challenge human's intuition and understanding of nature and become the emerging resources of quantum information technology. As a subtle supplement to entanglement and Bell nonlocality[1], Einstein-Podolsky-Rosen (EPR) steering[2] stands as a bridge between the two concepts. Entanglement as a vital quantum phenomenon is the most intrinsic feature of quantum mechanics with a variety of applications in continuous variable information processing[3], which has received widespread attention. And a great deal of effort has been devoted to generating and controlling entanglement[4–8]. The EPR steering, as a sufficient condition for entanglement, and a necessary condition for Bell nonlocality, was recognized by Schrödinger in 1935[9], and put on a firm mathematical footing by refs. [10,11]. Importantly, essentially different from entanglement and Bell nonlocality, the distinctive feature of EPR steering is intrinsically asymmetric between two observers[10,12]. The non-classical correlations in a bipartite scenario in which one of the parties can deduce the state that the other distant one holds according to the local measurement outcomes applied on the part of the entangled state in one side. No matter from the perspective of theory[2,13–22] or experiment[23–29], this feature makes quantum steering very important for various quantum information protocols that rely on entanglement by providing additional security[30], such as semisided device-independent quantum key distribution[31–33], quantum secret sharing[23,34], one-way quantum computing[35], subchannel discrimination[36], to name but a few. The quantum steering has been achieved in various systems, such as optomechanical systems[37,38], antiferromagnetic systems[23,39], and so on.

As we all know, most systems are inevitably coupled to environment via dissipation processes and the phenomenon of collective spontaneous radiation into the environment is so-called dissipative coupling[40]. It is an indirect coupling mechanism mediated by dissipative channels in open cavity systems. Specifically, the external dissipations of subsystems are non-trivial but correlated due to their interactions with the common reservoir[41]. In addition, the coherent coupling that stems from the direct dipole-dipole interaction is also ubiquitous in nature, it underpins a myriad of applications[42–44] and plays a crucial role in information processing technology. Intuitively, the coherently coupled subsystems exchange energy between each other periodically, which is determined by the coupling strength. This is different from the dissipatively coupled system, which is determined by the external dissipation strength.

In recent years, more attention has been focused on the physical study based on the coherent coupling and the dissipative coupling, we also note that the combination of coherent and incoherent manipulations was first widely used in atomic physics[45,46]. The dissipation-structured quantum self-organization predicts that the non-equilibrium initial state will 'drop' to metastable states in long-time limit, i.e., the entangled mixed states[47]. In physics, the classical interference between coherent coupling and dissipative coupling can induce one-way invisibility in the cooperative dissipation system[48]. Moreover, the quantum phenomenon induced by non-classical interference between two coupling ways is also fascinating. In the separated variable system, the selection of synergetic dissipation relative phase will dissipate the specific quantum state quickly (super-additive effect) and maintain its orthogonal state (subradiative effect)[47]. However, the relative phase dissipates the entanglement between subsystems in continuous variable systems, i.e., achieving one-way quantum steering.

Inspired by the previous research, in this paper, in light of the dissipation-coupled physics revealed in cavity magnonic systems, we propose a scheme to implement the controllable one-way steering by cooperative effect in a non-Hermitian cavity magnonic system involving photon and magnon modes. The one-way steering directivity depends only on the relative phase of cooperative dissipation and the frequency detuning of the magnon mode rather than the dissipations of subsystems, which

[1]Center for Quantum Sciences and School of Physics, Northeast Normal University, Changchun, Jilin 130024, China. [2]Department of Physics, College of Science, Yanbian University, Yanji, Jilin 133002, China. ✉email: hfwang@ybu.edu.cn; yixx@nenu.edu.cn

provides an effective method to generate and control the one-way steering instead of adding asymmetric losses or noises to subsystems at the cost of reducing steerability. Besides, the quantum correlation originating from the coherence between two coupling channels shows the robustness to environment temperature and the system dissipation. Furthermore, the entanglement can be obtained under the weak coherent coupling mechanism, as well as one-way steering can be obtained regardless of the strong coherent coupling mechanism or a large range of weak coherent coupling mechanism by adopting feasible experimental parameters.

RESULTS

Continuous variable open system

The physical model with cavity magnonics is depicted schematically in Fig. 1a, where a 1-mm diameter yttrium-iron-garnet (YIG) sphere is placed close to a cross-line microwave circuit. In the device, the circuit is designed to support both standing wave (coherent coupling) and traveling wave (dissipative coupling). In addition, the cavity and the YIG sphere are coupled to the same dissipative environment [Fig. 1b]. Here 'open' means that the external damping rate of the cavity is much larger than its intrinsic damping rate. The YIG sphere is glued to the end of a wooden stick, which is connected to a three-dimensional adjustable stage[48]. In our scheme, both the coherent coupling and the dissipative coupling can be drastically changed by moving the YIG sphere. In addition, a grounded loop antenna above the YIG sphere is used to control the damping rate of the magnon mode. The magnetic field of standing wave is shown in Fig. 1c, at the center of the cavity, the magnetic field strength is equal to zero, hence the coupling way is single dissipative coupling when the YIG sphere is local at the center of cross-line microwave circuit. The ratio between intrinsic damping and external damping of the magnon mode depends on the distance from the YIG sphere to the traveling wave cavity [Fig. 1d], i.e., dissipative coupling strength. When the distance is far, the energy radiated by the YIG sphere cannot be completely absorbed by the traveling wave cavity. On the contrary, once the YIG sphere is close to the traveling wave cavity, most of its spontaneously radiated energy can be dissipated into the microwave circuit. The device is placed inside a uniform magnetic field and the open cavity magnonic system is at the 20 mK temperature environment[49]. The non-Hermitian Hamiltonian of the whole system is

$$H/\hbar = \omega_c a^\dagger a + \omega_m b^\dagger b + (J - i\Gamma e^{i\theta})(a^\dagger b + a b^\dagger), \tag{1}$$

where $a^\dagger$ and $b^\dagger$ (a and b) are, respectively, the creation (annihilation) operators of the cavity mode with frequency ω_c and the magnon mode with frequency ω_m, satisfying standard commutation relations for bosons (see "Methods" section for the derivation of the effective Hamiltonian). In addition, the frequency of the magnon mode ω_m can be adjusted in a large range by the bias magnetic field **B** in the z direction with amplitude B_z via $\omega_m = \gamma_0 B_z$, where $\gamma_0/2\pi = 28$ GHz/T is the gyromagnetic ratio[7]. The parameter J (Γ) denotes the cavity-magnon coherent (dissipative) coupling rate, which can be modulated by varying the position of the YIG sphere above the microwave circuit[49]. Without losing generality, we choose the relative phase θ between the coherent and dissipative couplings as 0 and π for microwaves loaded from ports 1 and 2, respectively. In this case, the quantum Langevin equations for the operators in the system can be given by

$$\begin{aligned} \dot{a} &= -\kappa a - (\Gamma e^{i\theta} + iJ)b + \sqrt{2\kappa}a^{\mathrm{in}}, \\ \dot{b} &= -(i\Delta_m + \gamma)b - (\Gamma e^{i\theta} + iJ)a + \sqrt{2\gamma}b^{\mathrm{in}}, \end{aligned} \tag{2}$$

where $\Delta_m = \omega_m - \omega_c$ is the frequency detuning. Here $\kappa = \alpha + \kappa_{\mathrm{ex}}$ and $\gamma = \beta + \gamma_{\mathrm{ex}}$ are the dissipation rates of the photon and magnon modes, including the intrinsic (external) damping rates α and β (κ_{ex} and γ_{ex}), as well as the external dissipation rates are much larger than the intrinsic dissipation rates for two modes. Here, the external damping rates which induce the magnon-photon dissipative coupling are defined as $\Gamma = \sqrt{\kappa_{\mathrm{ex}}\gamma_{\mathrm{ex}}}$. The input noise operators o^{in} ($o = a, b$) are zero mean and are characterized by the following correlation functions: $\langle o^{\mathrm{in}\dagger}(t)o^{\mathrm{in}}(t')\rangle = n_o\delta(t-t')$ and $\langle o^{\mathrm{in}}(t)o^{\mathrm{in}\dagger}(t')\rangle = (n_o+1)\delta(t-t')$, where $n_o = (e^{\hbar\omega_o/k_BT}-1)^{-1}$ is the mean thermal excitation numbers in the environmental temperature T, with k_B being Boltzmann constant.

Exceptional points-like in model

In this part, we show that the coherent coupling and dissipative coupling play an important role in this scheme. The introduction of the dissipative coupling makes the Hermitian system become a $\mathcal{PT}$ symmetric non-Hermitian system. We display the real and imaginary parts of the eigenvalues for Hamiltonian in Eq. (1) as a function of the dissipative coupling strength Γ and the frequency detuning Δ_m in Fig. 2a, b. The real and imaginary parts of the eigenvalues of the Hamiltonian represent the eigenfrequency and dissipation rate of the two modes, respectively. Figure 2a shows that when the magnon-photon coherent coupling is not

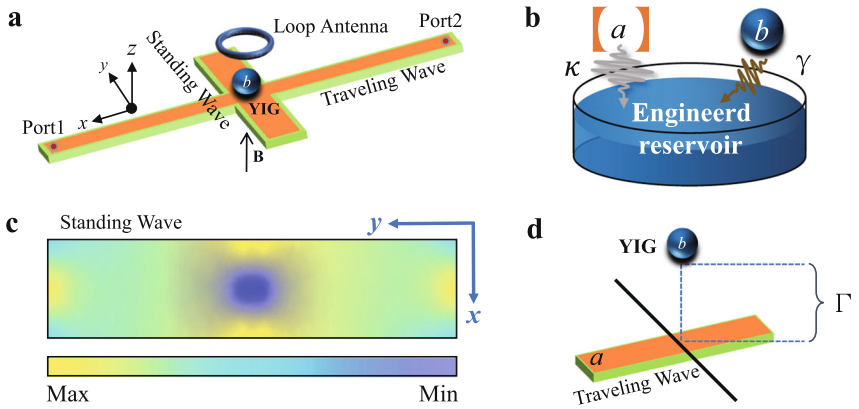

Fig. 1 Sketch of the open cavity magnonic system. a The yttrium-iron-garnet (YIG) sphere is placed inside a cross-line cavity which supports both standing wave and traveling wave. The entire experimental device is placed inside a uniform magnetic field, at the same time in the 20 mK temperature environment. **b** Both the cavity and the YIG sphere are coupled to the same dissipative environment. **c** The magnetic field strength and magnetic field distribution of the standing wave cavity. **d** The dissipative coupling strength can be adjusted by changing the distance between the YIG sphere and the cross-line circuit. The traveling wave is represented by a black line.

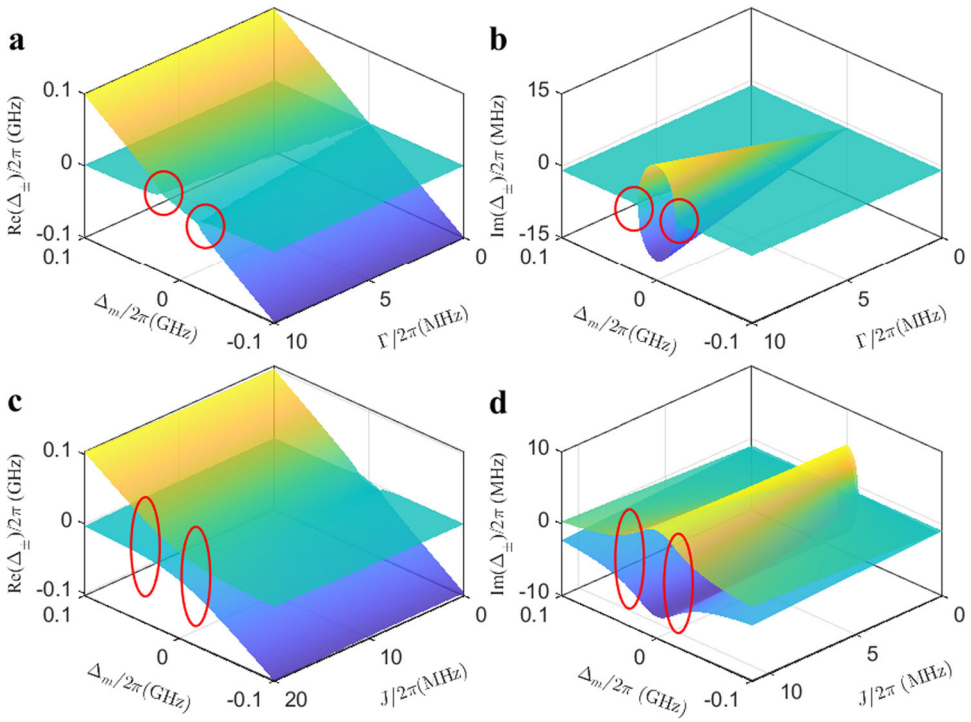

Fig. 2 Energy-level anti-crossing in the dissipative mechanism induced by coherent coupling. a, **c** Real parts and **b**, **d** imaginary parts of the eigenvalues of the Hamiltonian versus Δ_m, **a**, **b** Γ and **c**, **d** J. The parameters are set as $J/2\pi = 0$ in **a** and **b**, $\Gamma/2\pi = 6$ MHz in **c** and **d**, the other parameters are $\omega_c/2\pi = 10$ GHz, $\kappa/2\pi = \gamma/2\pi = 6$ MHz, $\alpha/2\pi = \beta/2\pi = 1$ MHz, $\theta = 0$, and $T = 20$ mK.

introduced into the system ($J = 0$) and in the absence of the dissipative coupling, the real and imaginary parts of the eigenvalues of the Hamiltonian show the standard eigenvalue energy spectrums of the Hermitian Hamiltonian. As the dissipative coupling strength increases, two EPs appear in the intrinsic energy spectrums, the real parts of the eigenvalues between the two EPs is degenerate and indistinguishable, and the imaginary parts of the eigenvalues dissipates separately into a superradiative state and a subradiative state[47], as shown in Fig. 2b. Nevertheless, when the magnon-photon coherent coupling is introduced, the strict EPs become EPs-like, as shown in Fig. 2c, d. As the coherent coupling strength increases with a fixed dissipative coupling rate, two EPs gradually disappear in the intrinsic energy spectrum, which is caused by the interference between the coherent coupling and dissipative coupling. Cearly, the real parts of the eigenvalues show the energy level repulsion in Fig. 2c, it is proved that the dominant coupling way is the magnon-photon coherent coupling. However, it is worth noting that the imaginary parts of the eigenvalues always split when the magnon-photon coherent coupling plays a dominant role [Fig. 2d], which is obviously different from the energy spectrum of the imaginary parts that only contain the dissipative coupling, therefore, the EPs (EPs-like) in Fig. 2a, b [Fig. 2c, d] are marked with red circles. In addition, both the EPs and EPs-like appear in two symmetrical positions in the case that the frequency detuning is close to zero. In the above discussion, one can see that the dissipative coupling and the coherent coupling are crucial in the scheme. Next, we will show detailedly the quantum interference between the two coupling ways can induce the quantum correlations between subsystems, such as quantum entanglement and quantum steering. Furthermore, the maximum correlation between subsystems which appears near two EPs-like are also confirmed.

Quantum interference induces quantum correlation

The foremost task of studying the properties of the entanglement and steering in cavity magnonic system is to find the optimal frequency detuning Δ_m, i.e., the optimal effective quantum interference between two coupling ways that can generate the entanglement and the steering. The entanglement between two modes can be quantified by the logarithmic negativity E_N arising from the covariance matrix (CM), and the one-way EPR steering can be quantified by $\mathcal{G}_{a\to b}$ or $\mathcal{G}_{b\to a}$. The calculation methods of these quantities are detailed in the "Methods" section. In order to observe the quantum correlations between subsystems more intuitively, we display the entanglement E_N, the one-way steering ($\mathcal{G}_{a\to b}$ and $\mathcal{G}_{b\to a}$), and the populations of modes in Fig. 3a–c, respectively, for microwaves loaded from port 1 ($\theta = 0$). Similarly, Fig. 3d–f corresponds to the case of $\theta = \pi$. We adopt experimentally feasible parameters: $\omega_c/2\pi = 10$ GHz, $\kappa/2\pi = \gamma/2\pi = 6$ MHz, $\kappa_{ex}/2\pi = \gamma_{ex}/2\pi = \Gamma/2\pi = J/2\pi = 5$ MHz, $\alpha/2\pi = \beta/2\pi = 1$ MHz, and low temperature $T = 20$ mK. In addition, the 1-mm diameter YIG sphere we considered has the total number of spins $N = \rho V \simeq 1.77 \times 10^{19}$, where V is the volume of the sphere and $\rho = 4.22 \times 10^{27}$ m^{-3} is the spin density of the YIG sphere[7]. All the results are obtained in the steady state guaranteed by the negative real parts of eigenvalues of the drift matrix (see the "Methods" section for details).

In order to make the description more convenient, we discuss the case of $\theta = 0$ in detail. Figure 3a shows that the magnon-photon entanglement E_N reaches the maximum when the frequency detuning between the magnon and photon modes is close to zero but not zero (near the EPs-like), and the entanglement E_N between the subsystems gradually increases for a greater dissipative coupling strength. In order to show the unidirectionality of the EPR steering more clearly, we plot the evolutions of the steerings $\mathcal{G}_{b\to a}$ and $\mathcal{G}_{a\to b}$, respectively, and merge them into Fig. 3b [This combined method is also applied to Fig. 3c, e, and f]. In the left half of Fig. 3b, we can clearly observe that under the current parameter conditions, the one-way steering $\mathcal{G}_{b\to a}$ completely occurs when the frequency detuning is negative. Similarly, in the right side of Fig. 3b, the one-way steering $\mathcal{G}_{a\to b}$ completely occurs when the frequency detuning is positive. In

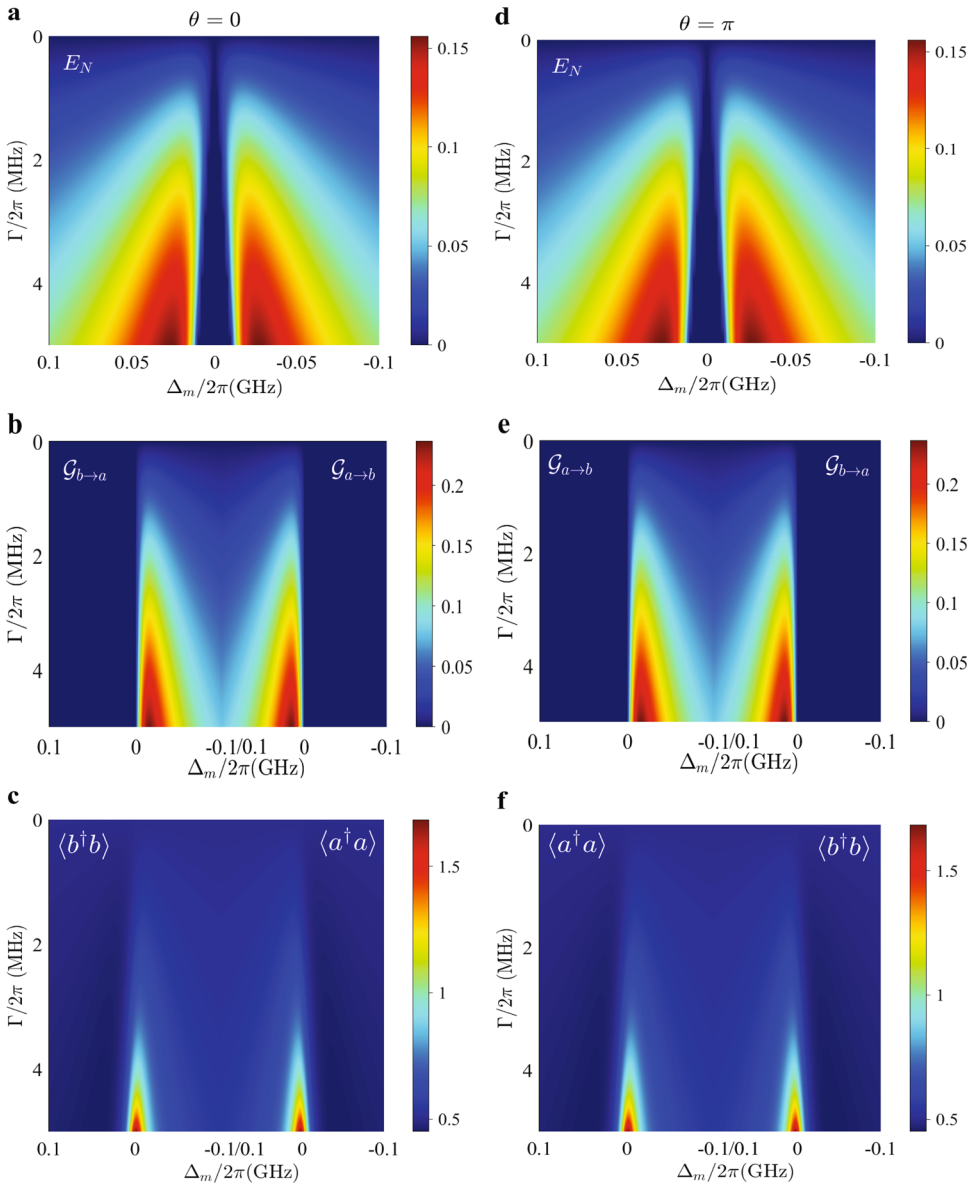

Fig. 3 Quantum correlations results. a, **b** Entanglement E_N, **b**, **e** steering ($\mathcal{G}_{b\to a}$ and $\mathcal{G}_{a\to b}$), **c**, **f** population of modes ($\langle b^\dagger b\rangle$ and $\langle a^\dagger a\rangle$) versus Δ_m and Γ for **a**–**c** $\theta = 0$ and **d**–**f** $\theta = \pi$, where $J/2\pi = 5$ MHz, the other parameters are the same as those in Fig. 2.

other words, in the evolution of EPR steering with the frequency detuning, the one-way steering $\mathcal{G}_{a\to b}$ and $\mathcal{G}_{b\to a}$ appear in positive frequency detuning and negative frequency detuning, respectively, that is, the EPR steering in the two directions no overlap at all. Therefore, the perfect one-way steering is achieved in our scheme. We also note that the quantum steering as a strict subset of entanglement has the similar properties to the entanglement in Fig. 3b. The one-way steering ($\mathcal{G}_{a\to b}$ or $\mathcal{G}_{b\to a}$), which is the same with the magnon-photon entanglement, reaches its maximum when there is a slight frequency detuning. Moreover, the optimal choice of the frequency detuning determines the direction of the one-way steering whose maximum value is greater than entanglement. In the previous studies, the degree of quantum entanglement is generally greater than EPR steering. This is due to that these schemes are always studied in the Hermitian systems[37–39,50], as well as the generations of quantum correlations in the previous studies rely on nonlinear effects, such as optomechanical interaction, Kerr nonlinearity, squeezed light, and more. However, compared to the previous studies, the quantum entanglement and EPR steering in our scheme are discussed in the non-Hermitian system. In addition, the strict EPs-like appear in the special non-Hermitian system, and the abundant quantum correlations occur near the EPs-like. Furthermore, the quantum correlations come from the quantum interference between the two coupling ways inside the non-Hermitian system, that is, the quantum correlations are generated by different mechanisms. The populations of modes is caused by the interference between the energy exchange channels are shown in Fig. 3c. In the left half of Fig. 3c, we can observe that the population of magnon mode $\langle b^\dagger b\rangle$ completely occurs when the frequency detuning is negative. Similarly, in the right side of Fig. 3c, the population of cavity mode $\langle a^\dagger a\rangle$ completely occurs when the frequency detuning is positive. Because of the selection of frequency detuning and the increase of the dissipative coupling, the magnon and photon modes exchange energy acutely, almost all of the particles converge on one of the modes, so only one mode has significant amount population. The generation of one-way steering can be explained by the population of subsystems, i.e., the fact is that the mode with a larger population is more

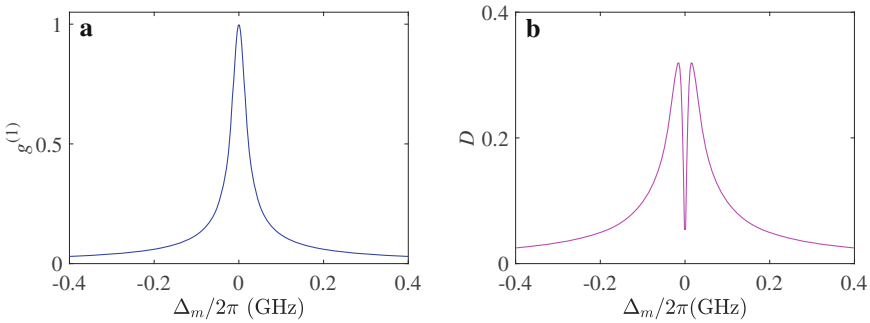

Fig. 4 Quantum coherence degree and indistinguishability. a First-order coherence degree $g^{(1)}$ and **b** indistinguishability D versus Δ_m for $\theta = 0$ or $\theta = \pi$. The corresponding parameters are $J/2\pi = 5$ MHz and $\Gamma/2\pi = 6$ MHz, and the other parameters are the same as those in Fig. 2.

difficult to steer by the other one. Consequently, the desired one-way steering can be achieved[8].

In the separated variable system, the relative phase of the coordinated dissipation between the subsystems can be understood as the decoherent phase. The initial state of the two individual qubits determines the coherence of the initial state of the system. If the phase of initial state coherence matches the phase of the dissipative channel, it will appear as a decoherence behavior with superradiation effect[47]. However, the relative phase of the coordinated dissipation in the continuous variable system is embodied as the decoherence behavior of the unilateral entangled state, i.e., one-way quantum steering. Figure 3d–f shows the variation of quantum correlations and the population of subsystems when the coordinated dissipation super-operator is changed from $\hat{o} = \hat{a} + \hat{b}$ to $\hat{o} = \hat{a} - \hat{b}$ (i.e., $\theta = 0 \to \theta = \pi$). Figure 3d shows that we can obtain the identical entanglement correlation when the propagation direction of the microwave is reversed. At this time, the direction of achievable one-way steering and the population of the relevant mode are reversed near the same EPs-like are shown in Fig. 3e, f, which means that the direction of the one-way steering in the coordinated dissipative open cavity magnonics system can be flexibly controlled by two key parameters, namely the frequency detuning Δ_m and the cooperative dissipation phase θ. The frequency detuning of the magnon mode can be adjusted by an external bias magnetic field, and the phase of the cooperative dissipation can be changed by varying the direction of traveling wave transmission[48]. It can be seen from quantum correlations that the present scheme has the following advantages: (i) the open cavity magnonic system has very flexible controllability; (ii) the generation of one-way steering adds no asymmetric losses or noises to the subsystems at the cost of reducing steerability, but changes the population of two modes through the interference between the energy exchange channels.

Next, in order to show the quantum coherence between the photon and magnon modes at the EPs-like, we utilize the first-order coherence function, which is defined as $g^{(1)} = (|\langle b^\dagger a\rangle|)/(\langle b^\dagger b\rangle^{1/2}\langle a^\dagger a\rangle^{1/2})$, to further analyze the reasons for the existence of quantum correlations, as shown in Fig. 4a. It shows that the cooperative effect between the coherent coupling and dissipative coupling is affected by the frequency detuning of the magnon mode. Similar to the classic case, we can classify the coherence according to the value of $g^{(1)}$. There are three different situations, namely $g^{(1)} = 1$, $0 < g^{(1)} < 1$, and $g^{(1)} = 0$, corresponding to first-order completely coherence, first-order partial coherence, and first-order completely irrelevance, respectively. We find that when the microwave cavity resonates with the YIG sphere ($\Delta_m = 0$), the first-order coherence degree $g^{(1)} = 1$, which implies the appearance of completely constructive interference. At the same time, the populations of the two modes $\langle a^\dagger a\rangle$ and $\langle b^\dagger b\rangle$ are equal, showing serious constructive interference [Fig. 3c, f], making the quantum correlations (entanglement and steering) decoherent [Fig. 3a, b, d, and e], i.e., $E_N = \mathcal{G}_{a\to b} = \mathcal{G}_{b\to a} = 0$. However, when there is a slight frequency detuning between the magnon and photon modes (near the EPs-like), the entanglement and one-way steering gradually appear, and both the populations of the two modes are always <1 ($\langle b^\dagger b\rangle < 1$, $\langle a^\dagger a\rangle < 1$), which is a prerequisite for generating the desired quantum correlations[8].

To further verify the obtained quantum correlation results, we introduce and plot the indistinguishability D, defined as $D = (|\langle b^\dagger b\rangle - \langle a^\dagger a\rangle|)/(\langle b^\dagger b\rangle + \langle a^\dagger a\rangle)$[50], as shown in Fig. 4b. Physically, the $g^{(1)} = 0$ means that there is no interference effect, and $D = 0$ means that the two subsystems are completely separable. On the contrary, when the value of D increases, i.e., there is a slight frequency detuning, it proves that the two subsystems are more indistinguishable. The above results indicate the reasons why the cooperative dissipation can induce quantum correlations in the open cavity magnonics system, i.e., the quantum correlations are caused by the interference between the two coupling ways near the EPs-like. In other words, both the quantum entanglement and one-way steering can be derived from the cooperative effect between the two coupling ways. This is clearly shown in Fig. 3, where the cavity-magnon entanglement and the quantum steering are equal 0, and the populations of the two modes are constant and equal when the dissipative coupling $\Gamma = 0$, by this time the two modes are not dissipated into the same environment.

Generally speaking, the coherent coupling has many different forms, such as weak coherent coupling, strong coherent coupling, even ultrastrong coherent coupling, etc. In contrast, since the dissipative coupling ($\Gamma = \sqrt{\kappa_{ex}\gamma_{ex}}$) is caused by the external dissipations of the two modes to the common reservoir, in which the coupling strength is always less than one or two dissipation rates. In such case, the dissipative coupling is always in a weak coupling mechanism ($\kappa, \gamma > \Gamma$) or in a magnetically induced transparency mechanism ($\kappa > \Gamma > \gamma$ or $\gamma > \Gamma > \kappa$)[51]. However, in general, the external dissipation is much larger than the internal dissipation. Therefore, it is meaningful to study the decoherence of quantum correlation from a general perspective. In order to make the cooperative effect between the coherent coupling and dissipative coupling sufficiently strong, while avoiding system asymmetry and the rapid decoherence of quantum effects caused by excessive single mode dissipation, we consider the case where the dissipation rates of the two modes are the same (i.e., $\kappa = \gamma \geq \Gamma$). To this end, we show the entanglement E_N and one-way steering $\mathcal{G}_{a\to b}$ versus ξ, environment temperature T, and the coherent coupling strength J in Fig. 5, where $\xi = \kappa = \gamma = \Gamma$ and $\kappa_{ex} \gg \alpha$, $\gamma_{ex} \gg \beta$, the white contour curves in figures are the dividing lines for the existence of entanglement and steering, and the dotted blue lines are the dividing line between the strong coherent coupling and the weak coherent coupling mechanisms. Figure 5a shows that the entanglement characteristic is quite robust to the system dissipations and environment temperature. When the dissipation rates of the subsystems and the coherent coupling

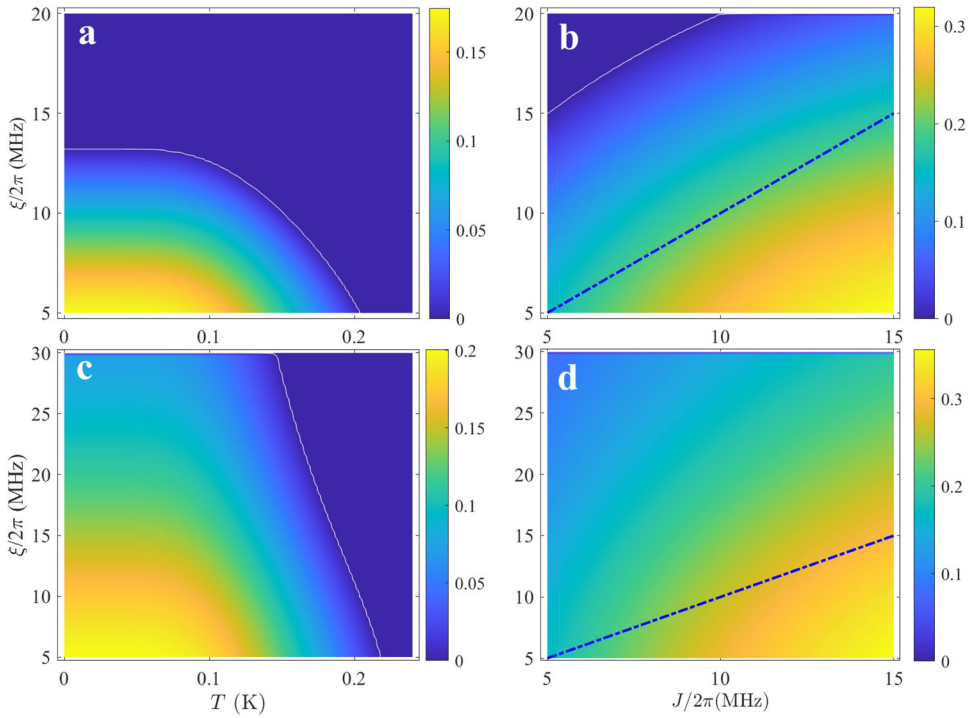

Fig. 5 Robust quantum entanglement and one-way steering. Entanglement E_N and steering versus ξ, **a**, **c** T and **b**, **d** J. The corresponding parameters are $J/2\pi = 5$ MHz in (**a**, **c**), $\xi = \kappa = \gamma = \Gamma$ in (**a**–**d**), and the other parameters are the same as those in Fig. 2, where the white contour lines depict the critical temperature and critical coherent coupling of entanglement and steering observability when the dissipation is fixed to a certain value.

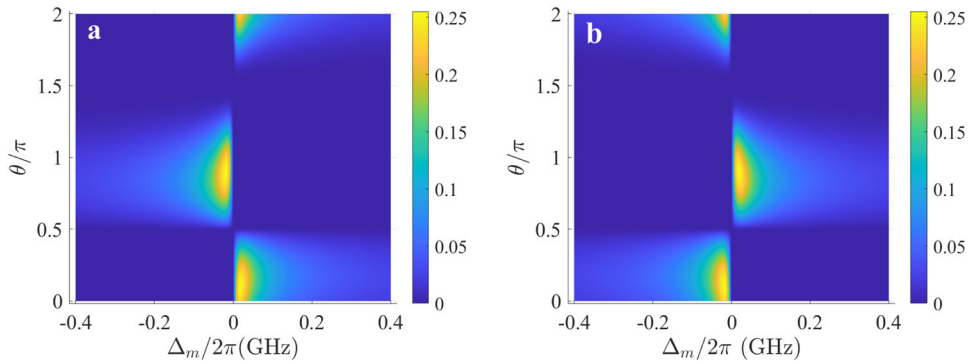

Fig. 6 Periodic asymmetric one-way steering. Quantum steering **a** $\mathcal{G}_{a\to b}$ and **b** $\mathcal{G}_{b\to a}$ as a function of the relative phase θ and frequency detuning Δ_m. The corresponding parameters are $J/2\pi = \Gamma/2\pi = 5$ MHz, and the other parameters are the same as those in Fig. 2.

parameter are relatively small, the entanglement is quite robust to the increase of environment temperature T, and within a certain range of dissipation parameters, the entanglement between the subsystems can be realized. However, once the dissipation parameter of the system is relatively large, approximately >13 MHz, no matter what the environment temperature is, the entanglement in the open cavity magnonic system cannot be achieved, that is the so-called entanglement sudden death phenomenon. In addition, the steering $\mathcal{G}_{a\to b}$ has the similar evolution characteristics compared to entanglement under the same parameter condition, as shown in Fig. 5c. It graphically shows that for larger system dissipation parameters, we can still achieve ideal one-way steering $\mathcal{G}_{a\to b}$. We can achieve the strong entanglement between the subsystems under the strong coherent coupling mechanism, and also can achieve a certain degree of correlation between subsystems under the weak coherent coupling mechanism, which is shown in Fig. 5b. Similarly, it also exhibits the entanglement sudden death phenomenon when the dissipation strength of system is approximately greater than 15 MHz. Figure 5d also shows that we can achieve the one-way steering $\mathcal{G}_{a\to b}$ regardless of the strong coherent coupling mechanism or a large range of weak coherent coupling mechanism. It is worth noting that we do not describe the steering $\mathcal{G}_{b\to a}$ in this part, because it is nonexistent under this parameter condition, which proves the feasibility of perfect asymmetric one-way steering.

Without loss of generality, we plot the measures of quantum steerings $\mathcal{G}_{a\to b}$ and $\mathcal{G}_{b\to a}$ as functions of the relative phase θ and frequency detuning Δ_m, as shown in Fig. 6. It clearly shows that the maximum value for one-way steering appears when there is a slight frequency detuning, which exactly corresponds to the results of Fig. 3b, e. Apparently, the one-way steering evolves with π periodically, maximized at phase $\theta \approx n\pi$ ($n \in \mathbb{Z}$) and minimized at $\theta \approx (n + 1/2)\pi$. Interestingly, the steering in two directions behaves asymmetrically with phase, i.e., the steering from mode a to mode b quantified by the parameter $\mathcal{G}_{a\to b}$ exhibits the phase-dependent

behavior, where steering in the other direction measured by the parameter $\mathcal{G}_{b\to a}$ behaves completely opposite result. Overall, Fig. 6 demonstrates that the coherent competition between the two couplings determines the unidirectionality of information transfer. This provides an active method to manipulate the steering directivity instead of adding asymmetric losses or noises to subsystems at the cost of reducing steerability.

DISCUSSION

In conclusion, we have proposed a way to achieve the controllable one-way quantum steering with strong entanglement in a non-Hermitian open cavity magnonic system. The one-way steering is the result of unilateral entanglement being dissipated induced by the cooperative effect. We use the cooperative dissipation to induce a unilateral quantum correlation between the two subsystems, which is different from the previous research on one-way steering that adds asymmetric losses or noises to subsystems at the cost of reducing steerability. The steering directivity can be controlled by the relative phase of the cooperative dissipation and the frequency detuning of the magnon mode. Furthermore, we also analyze the quantum entanglement sudden death phenomenon caused by the collective dissipation and the environment temperature, as well as the generation of the quantum entanglement and one-way steering under the weak coherent coupling mechanism and a range of the strong coherent coupling mechanism. Without loss of generality, we also discuss the effect of the relative phase θ on one-way steering. Our scheme is experimentally feasible and may promote to understand the asymmetric quantum correlation behavior in open cavity magnonic system, which has potential applications in semisided device-independent quantum key distribution, quantum secret sharing, one-way quantum computing, and subchannel discrimination, etc.

METHODS

Effective Hamiltonian of the coupled systems

When the interaction between cavity mode and magnon mode only includes the coherent coupling, the Hamiltonian of the system is given by

$$H_c/\hbar = \omega_c a^\dagger a + \omega_m b^\dagger b + J(a + a^\dagger)(b + b^\dagger), \tag{3}$$

where $a^\dagger$ and $b^\dagger$ (a and b) are, respectively, the creation (annihilation) operators of the cavity mode with frequency ω_c and the magnon mode with frequency ω_m. The coherent coupling strength J is a real number that includes a beam-splitter interaction and a parametric amplification interaction. Under the rotating wave approximation, the Hamiltonian (3) can be written as

$$H_{\mathrm{RWA}}/\hbar = \omega_c a^\dagger a + \omega_m b^\dagger b + J\left(a^\dagger b + a b^\dagger\right). \tag{4}$$

When the collective dissipation is considered, the system can be described by the specific form of Lindblad master equation:

$$\frac{d}{dt}\rho = -\frac{i}{\hbar}[H_{\mathrm{RWA}}, \rho] + \eta\mathcal{L}[c]\rho + a\mathcal{L}[a]\rho + \beta\mathcal{L}[b]\rho, \tag{5}$$

where the standard dissipative super-operator $\mathcal{L}[s]$ is defined as:

$$\mathcal{L}[s]\rho = 2s\rho s^\dagger - s^\dagger s\rho - \rho s^\dagger s,\ s = \{a, b, c\}. \tag{6}$$

The second term of Eq. (5) describes the collective dissipation between the cavity mode and the magnon mode into the traveling wave with rate η, and the third and fourth terms represent the intrinsic damping of the cavity mode and magnon mode with rate α and β, respectively. The jump operator c is expressed as the superposition operator of cavity operator and the magnon operator, and it depends on which port the microwave is loaded into. It has the general form (from port 1)[40]:

$$c \equiv \lambda a + \xi b. \tag{7}$$

Here, the individual couplings of the cavity mode and magnon mode to the traveling wave characterized by the coefficients λ and ξ satisfying $\eta\cdot\lambda^2 = \kappa_{\mathrm{ex}}$ and $\eta\cdot\xi^2 = \gamma_{\mathrm{ex}}$, which lead to the dissipative magnon-photon coupling. Furthermore, we can easily obtain the dissipative coupling between the two modes, which can be expressed as $\eta\cdot\lambda\xi = \sqrt{\kappa_{\mathrm{ex}}\gamma_{\mathrm{ex}}}$[47,48]. The quantum Langevin equations governing the dynamical behavior of the system are given by

$$\begin{aligned}\frac{d}{dt}a &= -i\omega_c a - (\alpha + \kappa_{\mathrm{ex}})a - (iJ + \sqrt{\kappa_{\mathrm{ex}}\gamma_{\mathrm{ex}}})b,\\ \frac{d}{dt}b &= -i\omega_m b - (\beta + \gamma_{\mathrm{ex}})b - (iJ + \sqrt{\kappa_{\mathrm{ex}}\gamma_{\mathrm{ex}}})a.\end{aligned} \tag{8}$$

According to these two equations, the effective dissipative coupling strength between cavity mode and magneton mode is $-i\Gamma = -i\sqrt{\kappa_{\mathrm{ex}}\gamma_{\mathrm{ex}}}$ clearly can be seen. However, when the microwave is loaded via port 2, the jump operator becomes $c \equiv \lambda a - \xi b$, in the same way, the effective dissipative coupling becomes $i\Gamma = i\sqrt{\kappa_{\mathrm{ex}}\gamma_{\mathrm{ex}}}$. We introduce the phase θ to represent the inclusion of both propagation directions, the effective non-Hermitian Hamiltonian of the coupled system containing the coherent coupling and dissipative coupling can be rewritten as:

$$H/\hbar = \widetilde{\omega}_c a^\dagger a + \widetilde{\omega}_m b^\dagger b + \left(J - ie^{i\theta}\Gamma\right)\left(a^\dagger b + a b^\dagger\right), \tag{9}$$

where $\widetilde{\omega}_c = \omega_c - i\alpha$ and $\widetilde{\omega}_m = \omega_m - i\beta$ represent the complex eigenvalues of the uncoupled cavity and magnon modes. For the convenience of subsequent descriptions, we use ω_c to represent $\widetilde{\omega}_c$ in the preceding part of the text.

Entanglement and steering

To quantify the entanglement and steering between the magnon and photon modes, we introduce two sets of quadrature components $X_a^{(\mathrm{in})}, Y_a^{(\mathrm{in})}, X_b^{(\mathrm{in})}$, and $Y_b^{(\mathrm{in})}$, which are defined as $\sqrt{2}X_o^{(\mathrm{in})} = o^{(\mathrm{in})} + o^{(\mathrm{in})\dagger}$ and $i\sqrt{2}Y_o^{(\mathrm{in})} = o^{(\mathrm{in})} - o^{(\mathrm{in})\dagger}$. Then, the linearized Langevin equations can be written in the compact matrix form,

$$\dot{\sigma}(t) = \mathcal{A}\sigma(t) + \varrho(t), \tag{10}$$

with $\sigma = [X_a, Y_a, X_b, Y_b]^T$ and $\varrho = [\sqrt{2\kappa}X_a^{\mathrm{in}}, \sqrt{2\kappa}Y_a^{\mathrm{in}}, \sqrt{2\gamma}X_b^{\mathrm{in}}, \sqrt{2\gamma}Y_b^{\mathrm{in}}]^T$ being the vectors of quantum fluctuations and noises, respectively. The drift matrix $\mathcal{A}$ reads

$$\mathcal{A} = \begin{pmatrix} -\kappa & 0 & \Gamma_\pm & J \\ 0 & -\kappa & -J & \Gamma_\pm \\ \Gamma_\pm & J & -\gamma & \Delta_m \\ -J & \Gamma_\pm & -\Delta_m & -\gamma \end{pmatrix}, \tag{11}$$

with $\Gamma_\pm \equiv \pm\Gamma$ for $\theta = \pi(0)$. Due to the linearity of the Langevin equations and Gaussian nature of the quantum noises, the system will decay to a stationary Gaussian state, which can be completely characterized by a 4×4 covariance matrix (CM) $\mathcal{V}$ in the phase space $\mathcal{V}_{ij} = \langle\sigma_i(t)\sigma_j(t') + \sigma_j(t')\sigma_i(t)\rangle/2$ $(i,j = 1,2,3,4)$. The steady-state CM $\mathcal{V}$ can be obtained straightforwardly by solving the Lyapunov equation,

$$\mathcal{A}\mathcal{V} + \mathcal{V}\mathcal{A}^T = -\mathcal{D}, \tag{12}$$

with $\mathcal{D}_{ij}\delta(t - t') = \langle\varrho_i(t)\varrho_j(t') + \varrho_j(t')\varrho_i(t)\rangle/2$.

The coherence between subsystems in the separated variable system is characterized by the off-diagonal elements of the density matrix[47]. However, for the continuous variable two-mode Gaussian state, a computable criterion of quantum steering based on quantum coherent information has been introduced[12]. While for quantum entanglement, it is convenient to use the logarithmic negativity E_N to quantify its level[52]. Note that all the above-mentioned measures can be computed from the 4×4 CM for the photon and magnon modes

$$\mathcal{V} = \begin{pmatrix} \mathcal{V}_1 & \mathcal{V}_3 \\ \mathcal{V}_3^T & \mathcal{V}_2 \end{pmatrix}, \tag{13}$$

where $\mathcal{V}_1$, $\mathcal{V}_2$, and $\mathcal{V}_3$ are 2×2 sub-block matrices of $\mathcal{V}$. In this case, the logarithmic negativity E_N between subsystems is expressed as

$$E_N \equiv \max[0, -\ln(2\nu)], \tag{14}$$

where $\nu = \sqrt{\mathcal{E} - (\mathcal{E}^2 - 4\mathcal{R})^{1/2}}/\sqrt{2}$ and $\mathcal{E} = \mathcal{R}_1 + \mathcal{R}_2 - 2\mathcal{R}_3$ with $\mathcal{R}_1 = \det\mathcal{V}_1$, $\mathcal{R}_2 = \det\mathcal{V}_2$, $\mathcal{R}_3 = \det\mathcal{V}_3$, and $\mathcal{R} = \det\mathcal{V}$ being symplectic invariants. And the Gaussian quantum steering is given by[14]

$$\begin{aligned}\mathcal{G}_{a\to b} &\equiv \max\left[0, \tfrac{1}{2}\ln\tfrac{\mathcal{R}_1}{4\mathcal{R}}\right],\\ \mathcal{G}_{b\to a} &\equiv \max\left[0, \tfrac{1}{2}\ln\tfrac{\mathcal{R}_2}{4\mathcal{R}}\right].\end{aligned} \tag{15}$$

Stability conditions of system

In general, the solution of the system will reach a steady state after a transient state relating to the initial conditions. If all the eigenvalues of the drift matrix $\mathcal{A}$ possess negative real parts, the system is stable and reaches a steady state. The stability conditions can be explicitly derived, e.g., by means of the Routh-Hurwitz criteria[53]. Therefore, we start our analysis by determining the eigenvalues of the matrix $\mathcal{A}$, i.e., $|\mathcal{A} - \lambda \mathbf{I}| = 0$, which yields the characteristic equation:

$$a_0\lambda^4 + a_1\lambda^3 + a_2\lambda^2 + a_3\lambda^1 + a_4\lambda^0 = 0, \tag{16}$$

where

$$a_0 = 1, \tag{17}$$

$$a_1 = 2(\gamma + \kappa), \tag{18}$$

$$a_2 = 2J^2 + \gamma^2 - 2\Gamma^2 + \Delta_m^2 + 4\gamma\kappa + \kappa^2, \tag{19}$$

$$a_3 = 2\big(-\gamma\Gamma^2 + 2J\Gamma\Delta_m + \kappa(\gamma^2 - \Gamma^2 + \Delta_m^2) + \gamma\kappa^2 + J^2(\gamma + \kappa)\big), \tag{20}$$

$$a_4 = (J^2 + \Gamma^2)^2 + 2\kappa(J^2\gamma - \gamma\Gamma^2 + 2J\Gamma\Delta_m) + \kappa^2(\gamma^2 + \Delta_m^2). \tag{21}$$

We can obtain a 4×4 matrix M using the coefficients a_i, as below

$$M = \begin{bmatrix} a_1 & a_0 & 0 & 0 \\ a_3 & a_2 & a_1 & a_0 \\ 0 & a_4 & a_3 & a_2 \\ 0 & 0 & 0 & a_4 \end{bmatrix}. \tag{22}$$

Now we define T_k to be the determinant of the first k rows and k columns of the matrix M with $k = 0, 1, \ldots, 4$. If all $T_k > 0$, then our system is stable[53]. The specific forms of T_k are expressed as follows:

$$T_0 = a_0 > 0, \tag{23}$$

$$T_1 = a_1 > 0, \tag{24}$$

$$T_2 = a_1a_2 - a_3a_0 > 0, \tag{25}$$

$$T_3 = a_1a_2a_3 - a_0a_3^2 - a_1^2a_4 > 0, \tag{26}$$

$$T_4 = a_1a_2a_3a_4 - a_0a_3^2a_4 - a_1^2a_4^2 > 0. \tag{27}$$

Hence, the numerical simulations in the scheme satisfy all the stability conditions mentioned above.

DATA AVAILABILITY

The data that support the findings of this study are available from the corresponding author upon request.

CODE AVAILABILITY

The codes used for numerical analysis are available from the corresponding author upon request.

Received: 25 March 2022; Accepted: 16 August 2022;
Published online: 03 September 2022

REFERENCES

1. Brunner, N., Cavalcanti, D., Pironio, S., Scarani, V. & Wehner, S. Bell nonlocality. *Rev. Mod. Phys.* **86**, 419 (2014).
2. Skrzypczyk, P., Navascués, M. & Cavalcanti, D. Quantifying Einstein-Podolsky-Rosen steering. *Phys. Rev. Lett.* **112**, 180404 (2014).
3. Horodecki, R., Horodecki, P., Horodecki, M. & Horodecki, K. Quantum entanglement. *Rev. Mod. Phys.* **81**, 865 (2009).
4. Bai, C. H., Wang, D. Y., Zhang, S., Liu, S. T. & Wang, H. F. Modulation-based atom-mirror entanglement and mechanical squeezing in an unresolved-sideband optomechanical system. *Ann. Phys* **531**, 1800271 (2019).
5. Wang, T. et al. Temperature-resistant generation of robust entanglemen with blue-detuning driving and mechanical gain. *Opt. Express* **27**, 29581 (2019).
6. Bai, C. H., Wang, D. Y., Zhang, S., Liu, S. T. & Wang, H. F. Generation of strong mechanical-mechanical entanglement by pump modulation. *Adv. Quantum Technol.* **4**, 2000149 (2021).
7. Li, J., Zhu, S. Y. & Agarwal, G. S. Magnon-photon-phonon entanglement in cavity magnomechanics. *Phys. Rev. Lett.* **121**, 203601 (2018).
8. Yu, M., Shen, H. & Li, J. Magnetostrictively induced stationary entanglement between two microwave fields. *Phys. Rev. Lett.* **124**, 213604 (2020).
9. Schrödinger, E. Discussion of probability relations between separated systems. *Proc. Camb. Philos. Soc.* **31**, 555 (1935).
10. Wiseman, H. M., Jones, S. J. & Doherty, A. C. Steering, entanglement, nonlocality, and the Einstein-Podolsky-Rosen paradox. *Phys. Rev. Lett.* **98**, 140402 (2007).
11. He, Q. Y., Rosales-Zárate, L., Adesso, G. & Reid, M. D. Secure continuous variable teleportation and Einstein-Podolsky-Rosen steering. *Phys. Rev. Lett.* **115**, 180502 (2015).
12. Kogias, I., Lee, A. R., Ragy, S. & Adesso, G. Quantification of Gaussian quantum steering. *Phys. Rev. Lett.* **114**, 060403 (2015).
13. Olsen, M. K. & Bradley, A. S. Bright bichromatic entanglement and quantum dynamics of sum frequency generation. *Phys. Rev. A* **77**, 023813 (2008).
14. He, Q. Y. & Reid, M. D. Einstein-Podolsky-Rosen paradox and quantum steering in pulsed optomechanics. *Phys. Rev. A* **88**, 052121 (2013).
15. Wang, M., Gong, Q. H., Ficek, Z. & He, Q. Y. Role of thermal noise in tripartite quantum steering. *Phys. Rev. A* **90**, 023801 (2014).
16. Midgley, S. L. W., Ferris, A. J. & Olsen, M. K. Asymmetric Gaussian steering: when Alice and Bob disagree. *Phys. Rev. A* **81**, 022101 (2010).
17. Olsen, M. K. Asymmetric Gaussian harmonic steering in second-harmonic generation. *Phys. Rev. A* **88**, 051802(R) (2013).
18. Schneeloch, J. et al. Einstein-Podolsky-Rosen steering inequalities from entropic uncertainty relations. *Phys. Rev. A* **87**, 062103 (2013).
19. Evans, D. A. & Wiseman, H. M. Optimal measurements for tests of Einstein-Podolsky-Rosen steering with no detection loophole using two-qubit Werner states. *Phys. Rev. A* **90**, 012114 (2014).
20. Rosales-Zárate, L. et al. Decoherence of Einstein-Podolsky-Rosen steering. *J. Opt. Soc. Am. B* **32**, A82 (2015).
21. Bowles, J., Vértesi, T., Quintino, M. T. & Brunner, N. One-way Einstein-Podolsky-Rosen steering. *Phys. Rev. Lett.* **112**, 200402 (2014).
22. He, Q. Y., Gong, Q. H. & Reid, M. D. Classifying directional gaussian entanglement, Einstein-Podolsky-Rosen steering, and discord. *Phys. Rev. Lett.* **114**, 060402 (2015).
23. Armstrong, S. et al. Multipartite Einstein-Podolsky-Rosen steering and genuine tripartite entanglement with optical networks. *Nat. Phys.* **11**, 167 (2015).
24. Händchen, V. et al. Observation of one-way Einstein-Podolsky-Rosen steering. *Nat. Photon.* **6**, 596 (2012).
25. Qin, Z. Z. et al. Manipulating the direction of Einstein-Podolsky-Rosen steering. *Phys. Rev. A* **95**, 052114 (2017).
26. Sun, K. et al. Experimental quantification of asymmetric Einstein-Podolsky-Rosen steering. *Phys. Rev. Lett.* **116**, 160404 (2016).
27. Wollmann, S., Walk, N., Bennet, A. J., Wiseman, H. M. & Pryde, G. J. Observation of genuine one-way Einstein-Podolsky-Rosen steering. *Phys. Rev. Lett.* **116**, 160403 (2016).
28. Xiao, Y. et al. Demonstration of multisetting one-way Einstein-Podolsky-Rosen steering in two-qubit systems. *Phys. Rev. Lett.* **118**, 140404 (2017).
29. Tischler, N. et al. Conclusive experimental demonstration of one-way Einstein-Podolsky-Rosen steering. *Phys. Rev. Lett.* **121**, 100401 (2018).
30. Opanchuk, B., Arnaud, L. & Reid, M. D. Detecting faked continuous-variable entanglement using one-sided device-independent entanglement witnesses. *Phys. Rev. A* **89**, 062101 (2014).
31. Branciard, C., Cavalcanti, E. G., Walborn, S. P., Scarani, V. & Wiseman, H. M. One-sided device-independent quantum key distribution: Security, feasibility, and the connection with steering. *Phys. Rev. A* **85**, 010301(R) (2012).
32. Gehring, T. et al. Implementation of continuous-variable quantum key distribution with composable and one-sided-device-independent security against coherent attacks. *Nat. Commun.* **6**, 8795 (2015).
33. Walk, N. et al. Experimental demonstration of Gaussian protocols for one-sided device-independent quantum key distribution. *Optica* **3**, 634 (2016).
34. Kogias, I., Xiang, Y., He, Q. Y. & Adesso, G. Unconditional security of entanglement-based continuous-variable quantum secret sharing. *Phys. Rev. A* **95**, 012315 (2017).
35. Li, C. M. et al. Genuine high-order Einstein-Podolsky-Rosen steering. *Phys. Rev. Lett.* **115**, 010402 (2015).
36. Piani, M. & Watrous, J. Necessary and sufficient quantum information characterization of Einstein-Podolsky-Rosen steering. *Phys. Rev. Lett.* **114**, 060404 (2015).
37. ElQars, J., Daoud, M. & AhlLaamara, R. Controlling stationary one-way steering via thermal effects in optomechanics. *Phys. Rev. A* **98**, 042115 (2018).
38. Liao, C. G., Xie, H., Chen, R. X., Ye, M. Y. & Lin, X. M. Controlling one-way quantum steering in a modulated optomechanical system. *Phys. Rev. A* **101**, 032120 (2020).

39. Zheng, S. S., Sun, F. X., Lai, Y. J., Gong, Q. H. & He, Q. Y. Manipulation and enhancement of asymmetric steering via interference effects induced by closed-loop coupling. *Phys. Rev. A* **99**, 022335 (2019).
40. Metelmann, A. & Clerk, A. A. Nonreciprocal photon transmission and amplification via reservoir engineering. *Phys. Rev. X* **5**, 021025 (2015).
41. Wang, Y. P. & Hu, C. M. Dissipative couplings in cavity magnonics. *J. Appl. Phys.* **127**, 130901 (2020).
42. Wallquist, M., Hammerer, K., Rabl, P., Lukin, M. & Zoller, P. Hybrid quantum devices and quantum engineering. *Phys. Scr.* **T137**, 014001 (2009).
43. Kurizki, G. et al. Quantum technologies with hybrid systems. *Proc. Natl Acad. Sci. USA* **112**, 3866 (2015).
44. Xiang, Z. L., Ashhab, S., You, J. Q. & Nori, F. Hybrid quantum circuits: superconducting circuits interacting with other quantum systems. *Rev. Mod. Phys.* **86**, 623 (2013).
45. Beige, A. et al. Quantum computing using dissipation to remain in a decoherence-free subspace. *Phys. Rev. Lett.* **85**, 1762 (2000).
46. Pachos, J. & Walther, H. Quantum computation with trapped ions in an optical cavity. *Phys. Rev. Lett.* **89**, 187903 (2002).
47. Yang, Z. B., Wang, Y. P., Li, J., Hu, C. M. & You, J. Q. Entanglement emerges from dissipation-driven quantum self-organization. Preprint at https://arxiv.org/abs/2109.12315 (2021).
48. Wang, Y. P. et al. Nonreciprocity and unidirectional invisibility in cavity magnonics. *Phys. Rev. Lett.* **123**, 127202 (2019).
49. Yang, Y. et al. Unconventional singularity in anti-parity-time symmetric cavity magnonics. *Phys. Rev. Lett.* **125**, 147202 (2020).
50. Zheng, S. S. et al. Enhanced entanglement and asymmetric EPR steering between magnons. *Sci. China-Phys. Mech. Astron* **64**, 210311 (2021).
51. Zhang, D. K., Luo, X. Q., Wang, Y. P., Li, T. F. & You, J. Q. Observation of the exceptional point in cavity magnon-polaritons. *Nat. Commun.* **8**, 1368 (2017).
52. Vidal, G. & Werner, R. F. Computable measure of entanglement. *Phys. Rev. A* **65**, 032314 (2002).
53. DeJesus, E. X. & Kaufman, C. Routh-Hurwitz criterion in the examination of eigenvalues of a system of nonlinear ordinary differential equations. *Phys. Rev. A* **35**, 5288 (1987).

ACKNOWLEDGEMENTS

This work was supported by the National Natural Science Foundation of China under Grants No. 12074330, No. 11775048, and No. 12047566.

AUTHOR CONTRIBUTIONS

S.Y.G. and H.F.W. initiated the project and wrote the manuscript. H.F.W. and X.X.Y. provided expertise on the theoretical analysis. H.F.W. supervised the project. All authors discussed the results and contributed to the final manuscript.

COMPETING INTERESTS

The authors declare no competing interests.

ADDITIONAL INFORMATION

Correspondence and requests for materials should be addressed to Hong-Fu Wang or Xuexi Yi.

Reprints and permission information is available at http://www.nature.com/reprints

Publisher's note Springer Nature remains neutral with regard to jurisdictional claims in published maps and institutional affiliations.